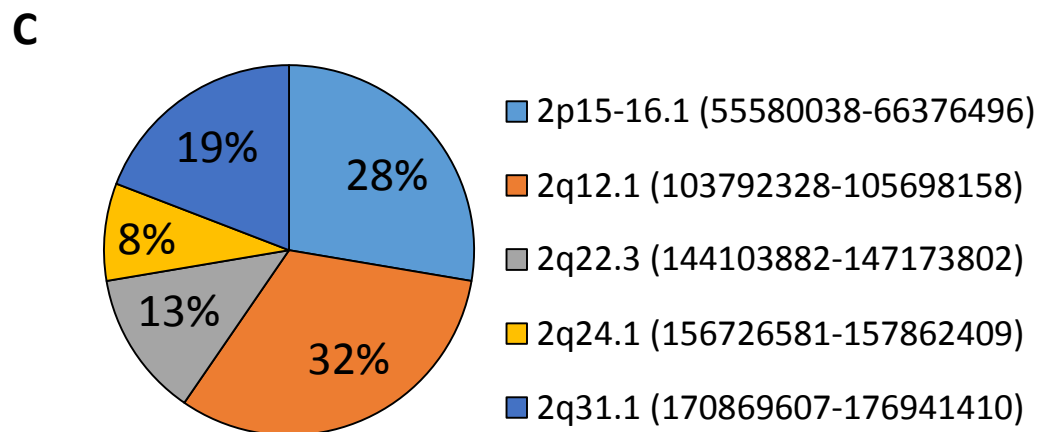
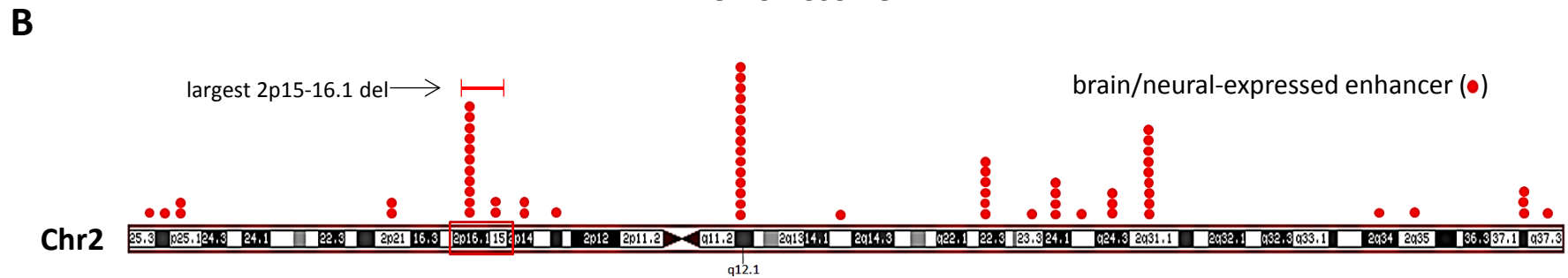
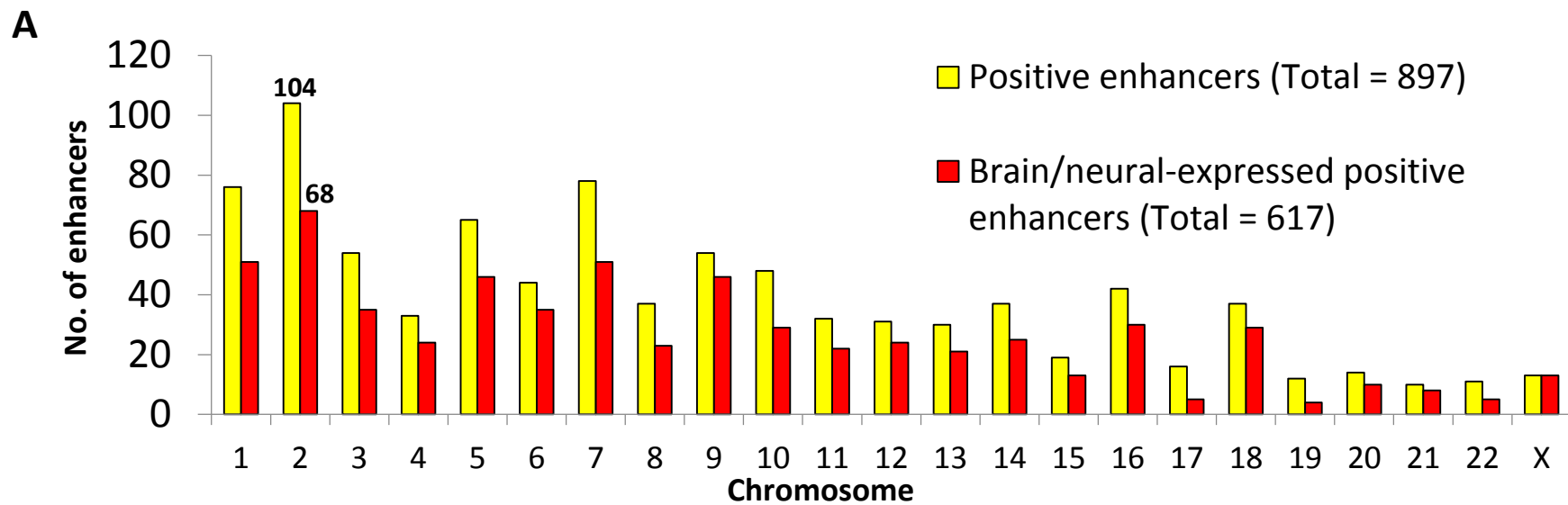


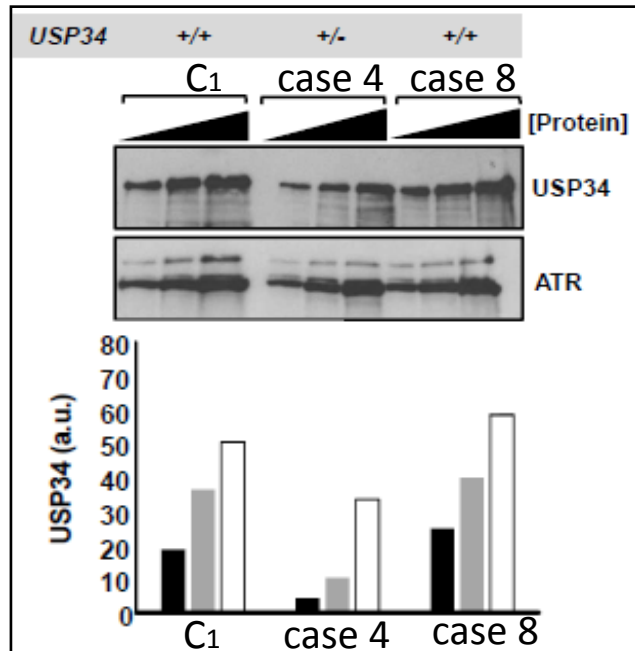
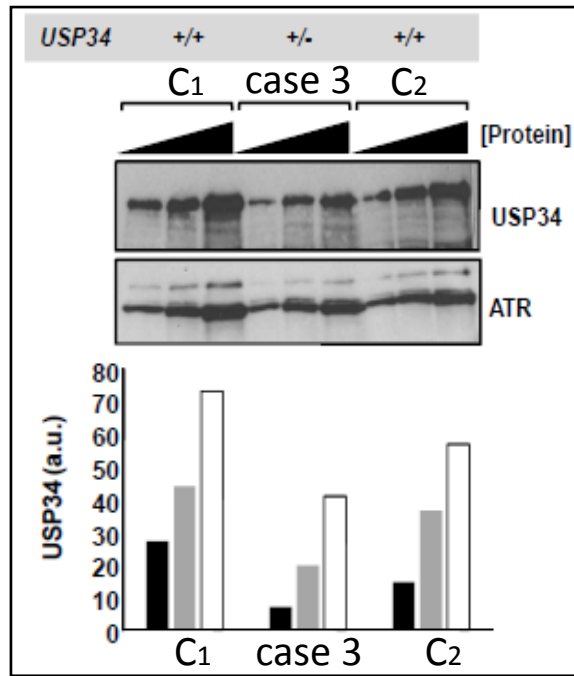
Supplemental Figure 1 – Three CNVs from 2p15p16.1 in case 2.

Case 2 had three 2p15p16.1 deletions: One large (~2Mb) and two additional smaller CNVs (~17Kb and ~27Kb). The red bars indicate the deletions. The detailed breakpoint junctions and positions of the two small CNVs (encircled) in relation to the large CNV are shown on the diagram: One CNV lied within the second intron of *BCL11A* (60700679-60717669) and adjacent to two *BCL11A* SNPs (indicated with yellow stars), rs1427407 (at 60,718,043) and rs75994488 (60,718,097-60,718,597), associated with fetal hemoglobin expression and neurodevelopment, respectively. The extent of the second CNV was refined with QMPSF (60828557-60855688) to show that it overlaps with enhancer 1142 which has a high expression in the hindbrain of the mouse (as reported by VISTA).

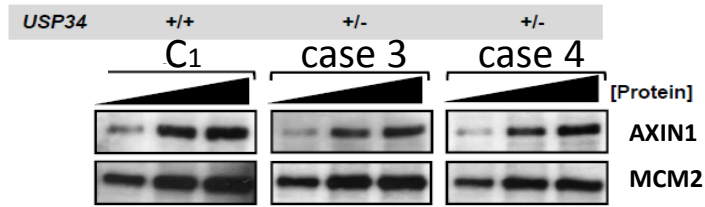


Supplemental Figure 2 – Distribution of enhancers among human chromosomes. A) Distribution of the total of 897 enhancers per chromosome. 104 positive enhancers and 68 brain/neural-expressed enhancers are on chromosome 2. B) Distribution of all 68 brain/neural-expressed enhancers on chromosome 2 cytotbands. The largest 2p15p16.1 deletion which was found in our newly recruited case 1 (chr2:55676099-65250541, hg19) is shown with a red scale-bar which covers all the 13 enhancers in that region distributed in chr2:58748340-63277103). C) The percentage enrichment of top 5 enriched chromosome 2 cytotbands with brain/neural-expressed enhancers. The top 5 enriched cytotbands were identified based on if they harbored at least 4 brain/neural-expressed enhancers. Almost a third of brain/neural-expressed enhancers on chromosome 2 are enriched at 2p15p16.1.

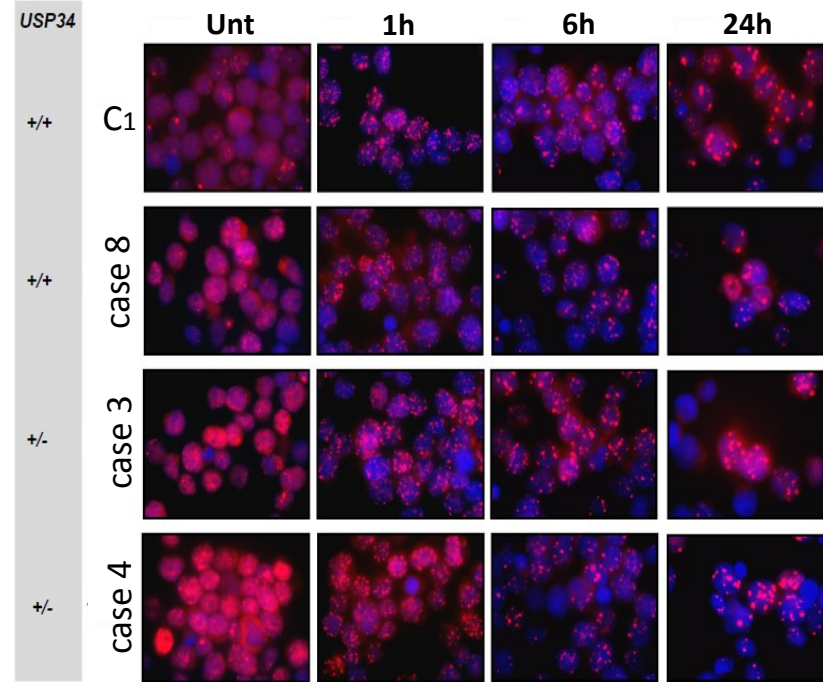
A



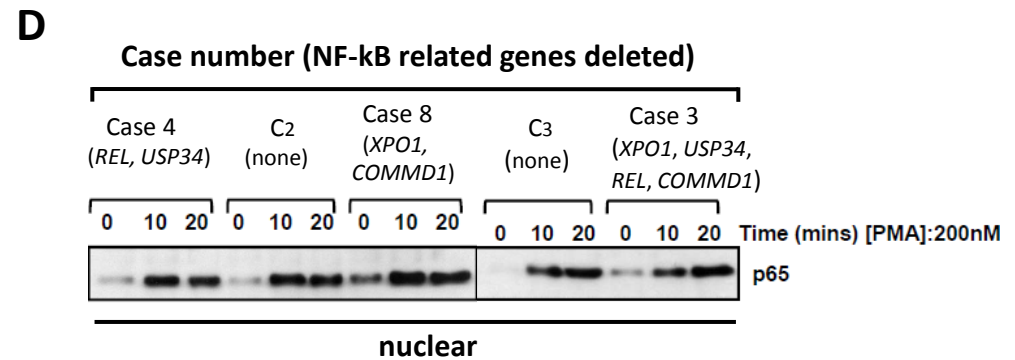
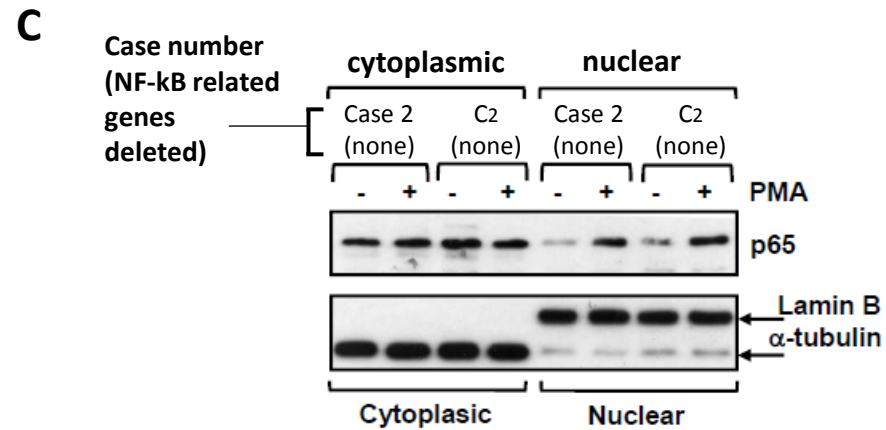
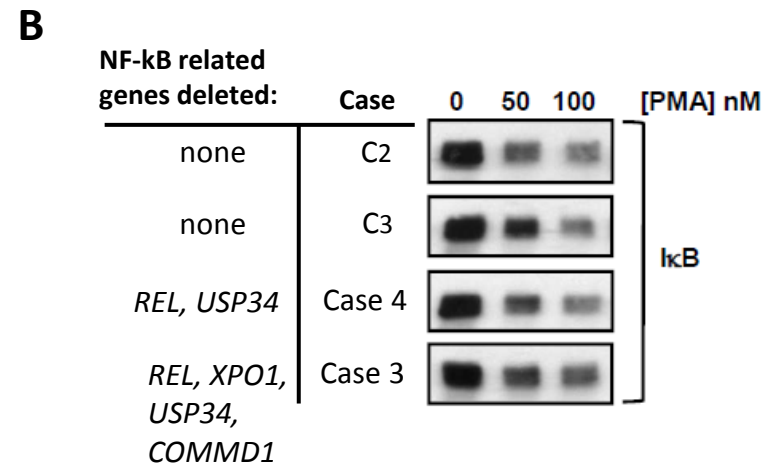
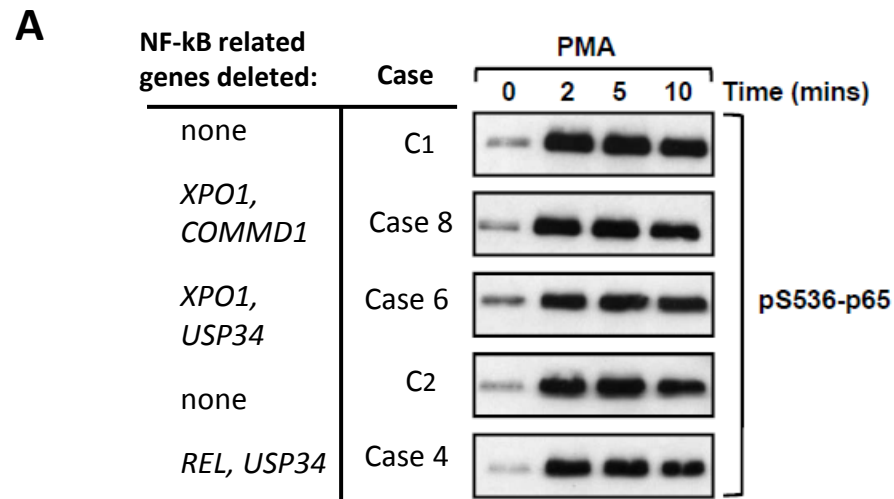
B



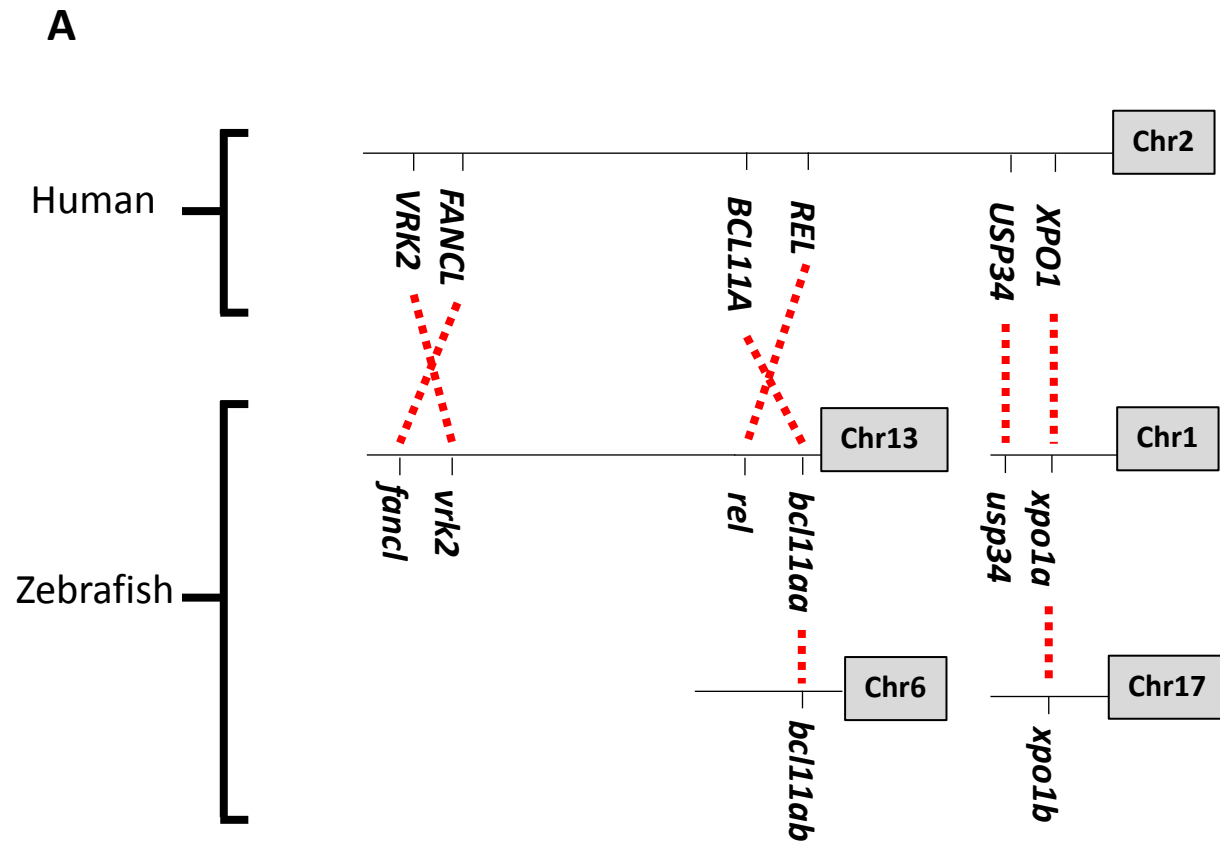
C



Supplemental Figure 3 – Haploinsufficiency of *USP34* is associated with reduced *USP34* expression. A) *USP34* expression was assessed by titrating increasing concentrations of whole-cell extracts (WCE) (50mg, 100mg, 200mg) from control and patient LCLs. Antibodies against ATR confirmed equal loading. Case 3 and 4 with *USP34* deletion exhibit approximately 50% reduction in *USP34* expression. Quantification was performed using Image J. B) Increasing amounts of WCE prepared from LCLs with differing *USP34* copy number were probed with AXIN1. MCM2 antibody confirmed equal loading. C) LCLs were either untreated (Unt) or irradiated with 3Gy ionizing radiation (IR) and 53BP1 foci formation monitored at different times post-irradiation. 53BP1 foci are used as a marker of double-strand breaks (DSBs) and can be used to assess double-strand break repair (DSB-R) capacity. IR-induced 53BP1 foci form and dissipate over time post-irradiation in LCLs with normal *USP34* copy number (C_1 and case 8) similar to those with *USP34* deletion (case 3 and 4). Images were acquired at 40x magnification using the Zeiss Axioplan platform and SimplePCI software. C_1 = Control; $+/+$ = presence of both copies; $+/-$ = Deletion of one copy (heterozygous)



Supplemental Figure 4 – NF- κ B pathway analysis in patient cell-lines. A) Phosphorylation of the NF- κ B family transcription factor p65/RelA on serine 536 (pS536-p65) was assessed at different times in patient lymphoblast cell lines (LCLs) with differing deletions of NF- κ B related genes following treatment with 200nM Phorbol 12 Myristate 13-Acetate (PMA) to induce NF- κ B pathway. Phosphorylation was induced and maintained equally in control cells (C₁ and C₂) with normal copy number of NF- κ B related genes compared to case 4 (with *REL* and *USP34* deletion), case 6 (with *XPO1* and *USP34* deletion), and case 8 (with *XPO1* and *COMMD1* deletion). B) NF- κ B pathway activation occurs via phosphorylation and consequent ubiquitin-mediated degradation of IkB which enables the nuclear translocation of NF- κ B family transcription factors. We assessed the kinetics of PMA-induced IkB degradation in patient LCLs with differing deletions of NF- κ B related genes. LCLs were treated with increasing concentrations of PMA for 10 mins. IkB was degraded similarly and effectively in LCLs with normal NF- κ B copy number (controls, C₂ and C₃) compared to those with a deletion of NF- κ B related genes; case 3 (with *REL*, *XPO1*, *USP34*, and *COMMD1* deletion) and case 4 (with *REL* and *USP34* deletion). C) The penultimate step of NF- κ B pathway involves the nuclear translocation of activated NF- κ B family transcription factors where they regulate expression of their target genes. We assessed PMA-mediated nuclear translocation of p65/RelA by fractionating various LCLs into cytoplasmic and nuclear extracts. LCLs from a control (C₂) and case 2, which had no NF- κ B related genes deleted, when treated with PMA (200nM 10mins), showed marked increase in p65 levels in the nuclear fraction. The quality of the fractionation was assessed by reciprocal blotting for expression of a nuclear protein (Lamin B) and a cytoplasmic protein (α -tubulin). D) Nuclear translocation was assessed in control LCLs (C₂ and C₃) lacking NF- κ B related gene deletions and case 3 (with *XPO1*, *USP34*, *REL*, and *COMMD1* deleted), case 4 (with *REL* and *USP34* deleted), and case 8 (with *XPO1* and *COMMD1* deleted) following treatment with 200nM PMA at the times indicated. PMA-induced nuclear recruitment of p65 was unaffected by the copy number of indicated NF- κ B related genes.

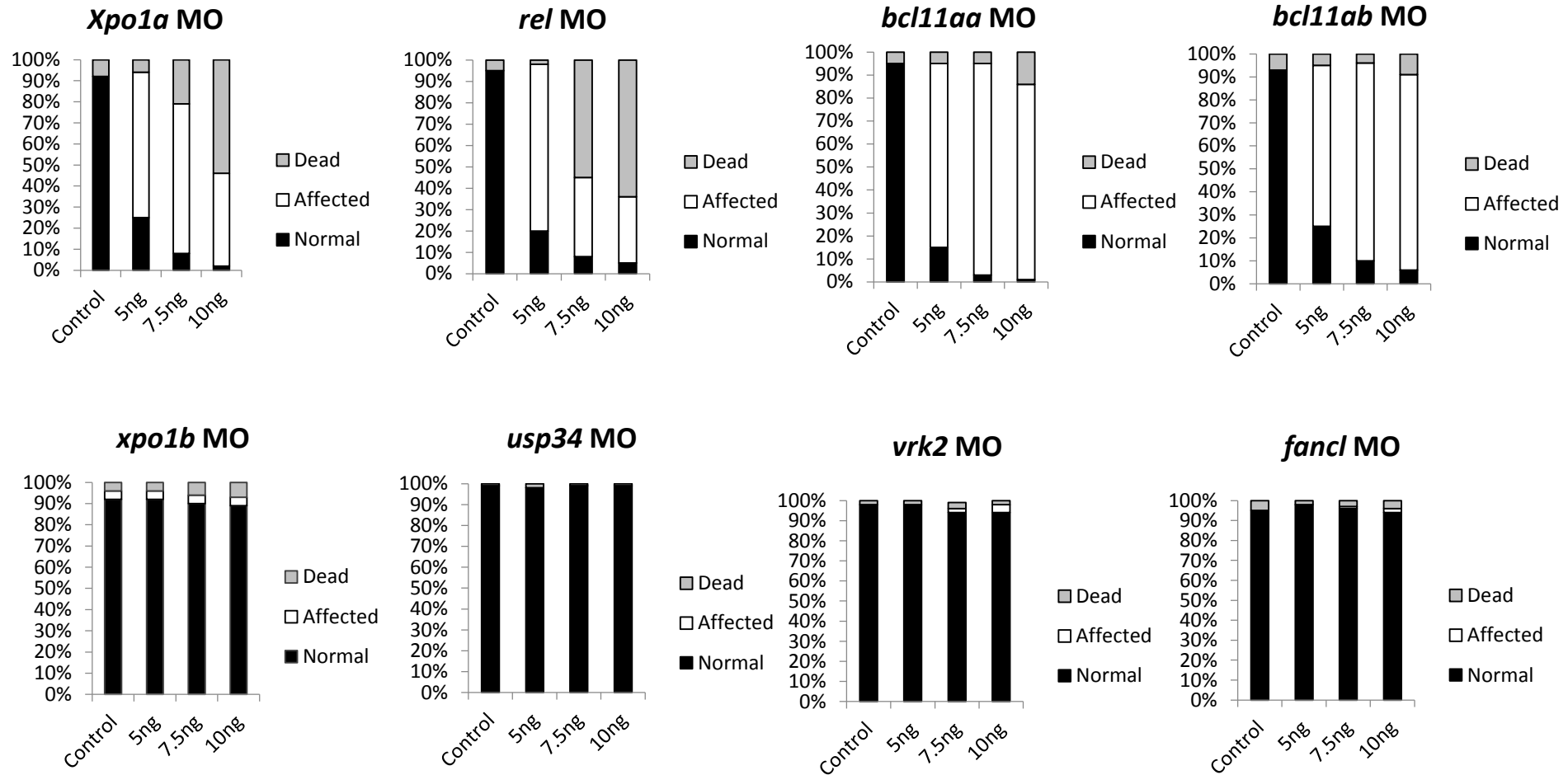


B

Human gene	Zebrafish orthologue	% Protein homology
	<i>xpo1b</i>	90
<i>REL</i>	<i>rel</i>	51
	<i>bcl11ab</i>	64
<i>FANCL</i>	<i>fancl</i>	58

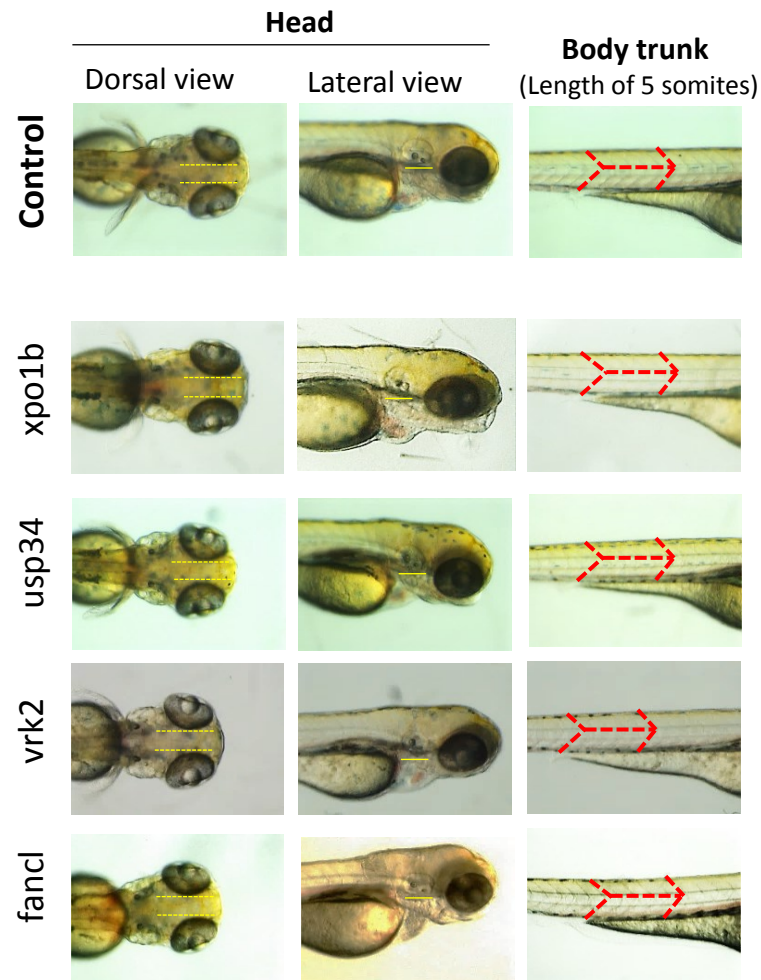
Supplemental Figure 5 – 2p15p16.1 gene synteny and protein homology in human versus zebrafish.

A) Location of 2p15p16.1 genes in relation to each other extracted from the UCSC genome browser and Ensembl database. B) *XPO1* and *BCL11A* genes have two orthologous copies in zebrafish: (*xpo1a*, *xpo1b*) and (*bcl11aa*, *bcl11ab*), respectively. All other genes have a single zebrafish ortholog. The % protein homology of the genes were obtained by sequence alignment of human and zebrafish proteins using Clustal Omega Multiple Sequence Alignment web-tool (EMBL). *XPO1*, *USP34*, and *BCL11A* were the highly conserved genes with ~80-90% protein homology.

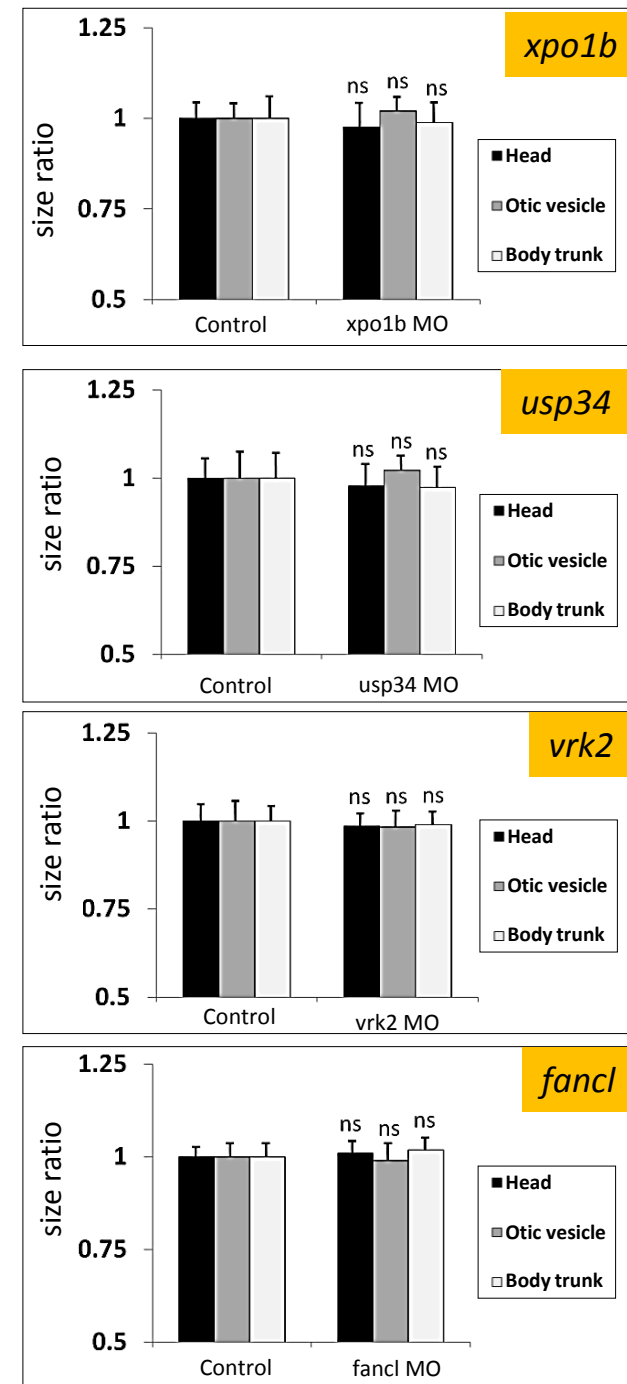


Supplemental Figure 6 – Morpholino titration analysis for 2p15p16.1 zebrafish orthologous genes.

Dose-response curve of *xpo1a*, *xpo1b*, *rel*, *usp34*, *bcl11aa*, *bcl11ab*, *vrk2*, and *fanc1* morpholinos (MOs) were obtained by injection of 1-2 cell stage wild-type zebrafish embryos with increasing concentrations of MOs (5ng, 7.5ng, and 10ng). The head and body size/structure of injected fish were compared with control embryos (injected with 10ng of gene-mismatch MOs) and the % of embryos with normal, affected, or dead phenotypes were scored at 3 days post-fertilisation (dpf).

A

Supplemental Figure 7 – No head and body abnormalities were detected for *xpo1b*, *usp34*, *vrk2*, and *fancl* morphants. A) Microscopic images and B) size measurements of the head (distance between the eyes), otic vesicle, and the body trunk (distance between 5 tail somites) of the 3 days post-fertilisation (dpf) embryos that were injected with *xpo1b*, *usp34*, *vrk2*, and *fancl* morpholinos (MOs). The size measurements were carried out with ImageJ software, normalized to the sizes obtained in controls and the ratios were plotted. No significant difference in the head, otic vesicle, and body size was noted in morphants versus controls. Images were acquired at 115x magnification. Data represented as Mean \pm S.D. from 3 independent injections. N=50 embryos per gene per injection. Student's t-test was used to determine the significance of the differences for measured sizes between each gene morphant and controls. ns = $p > 0.01$

B

A

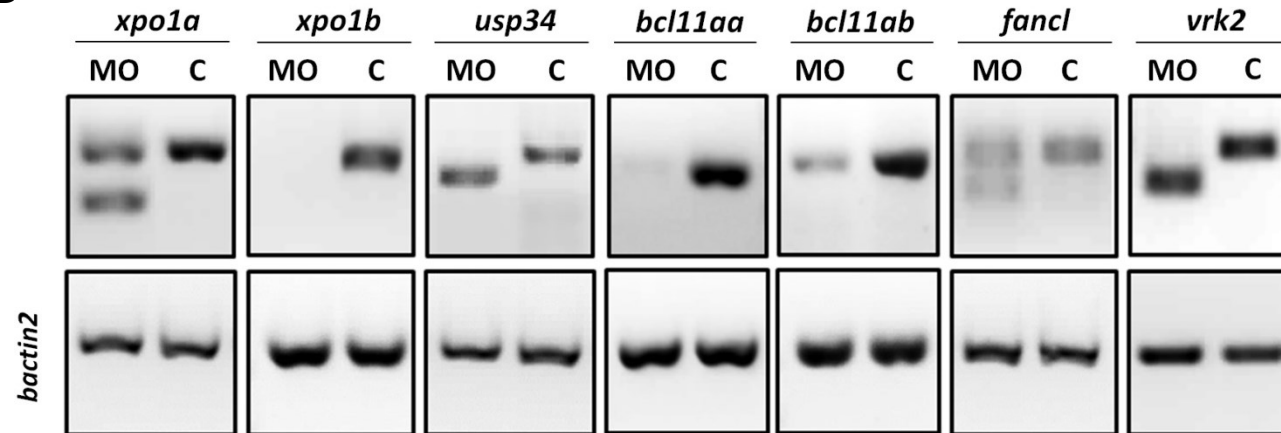
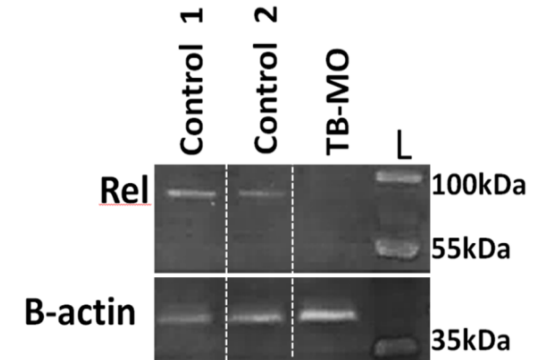
Zebrafish gene	SB-MO knockdown consequence	Amplified region with PCR (normal size)	Expected PCR products in MO vs MM
<i>xpo1a</i>	Exon 9 (129bp) deletion	e8-e11 (420 bp)	Absence/low normal PCR amplicon; presence of truncated product (291 bp)
<i>xpo1b</i>	Intron 1 (1999bp) inclusion	e1-e6 (464 bp)	Absence/low normal PCR amplicon; presence of larger product (2125 bp)
<i>rel</i> *	-	-	-
<i>usp34</i>	Exon 2 (119bp) deletion	e1-e3 (489 bp)	Absence/low normal PCR amplicon; presence of truncated product (370 bp)
<i>bcl11aa</i>	Intron 1 (3250bp) inclusion	5' UTR-e2 (363 bp)	Absence/low normal PCR amplicon; presence of larger product (3613 bp)
<i>bcl11ab</i>	Intron 1 (7226bp) inclusion	5' UTR-e2 (353 bp)	Absence/low normal PCR amplicon; presence of larger product (7579 bp)
<i>fancl</i>	Exon 3 (61bp) deletion	e1-e5 (297 bp)	Absence/low normal PCR amplicon; presence of truncated product (236 bp)
<i>vrk2</i>	Exon 4 (88bp) deletion	e2-e5 (300 bp)	Absence/low normal PCR amplicon; presence of truncated product (212bp)
<i>Actb2 (bactin2)**</i>	N/A	e4-e5 (322 bp)	Comparable levels of PCR product between MO vs MM

Abbreviations: SB-MO = Splice-blocking morpholino; MM = Mismatch control; N/A = Not applicable; e = exon; i = intron; F = Forward; R = Reverse; UTR = Untranslated region

§ Presence of large products (>1000 bp) were difficult to detect due to their large size, therefore we assessed the intensity of the normal PCR amplicon vs MM controls to confirm successful knock-down.

* *rel* knockdown was not successful with two independently designed splice-blocking morpholinos, therefore translation-blocking morpholino was used and knockdown was confirmed with western-blotting.

** primer sequences for *Actb2* were obtained from Casadei et al., (2011) (PMID: 21281742) and were used as the housekeeping gene control

B**C**

Supplemental Figure 8 – Confirmation of gene knockdown in zebrafish embryos by RT-PCR. A) Expected consequence of splice-blocking morpholino (SB-MO) knockdown on each gene transcript sequence and B) the agarose gel electrophoresis images of RT-PCR products from total RNA extracted from the morphant fish embryos. SB-MOs designed for each gene had specific exon-intron boundary target sites (as indicated). Primers surrounding the target site were designed to amplify the region of splice-blockage. All SB-MO injections (except for *rel*) successfully knocked-down the gene-of-interest, as was shown by change in the sequence, hence the size of the transcript, and/or intensity of the PCR product in comparison to controls. Equal loading was controlled with *bactin2*. C) For *rel*, we confirmed the gene knockdown by analysing the protein expression through western-blotting in translation-blocking morpholino (TB-MO) injected embryos.

Supplemental Table 2 – Breakpoints of 2p15p16.1 microdeletion in 33 cases.

Case	Chr	Start	End	Size		Gender	Inheritance	Platform	Additional reported genomic findings
Florisson et al. 2013 (1)	2	55,616,146	62,362,249	6,746,103	min del	Male	<i>de novo</i> , parental origin ND	Affymetrix 250K Nsp1 SNP array, fine mapping by qPCR	None reported
		55,580,038	62,416,010	6,835,972	bal				
Rajcan-Separovic et al. 2007 (2)	2	55,627,639	63,519,476	7,891,837		Male	<i>de novo</i> , paternal allele deleted	Affymetrix Genome-Wide Human SNP Array 6.0 (*)	Maternal del at 16p13.11 (1.1 Mb)
Case_1	2	55,676,099	65,250,541	9,574,442		Male	<i>de novo</i> , parental origin ND	Affymetrix CytoScan 750K Array, hg19	No additional pathogenic CNVs Reported
									Paracentric inversion of chromosome 7 and an apparently balanced translocation between chromosome 1 and 7, involving the inverted chromosome 7 [46,XX,der(7)inv(7)(q21.1q32.1)t(1;7)(q23q32.1)]
Prontera et al. 2011	2	56,853,162	60,380,981	3,527,819		Female	<i>de novo</i> , parental origin ND	Affymetrix Genome-Wide Human SNP Array 6.0	
Rajcan-Separovic et al. 2007 (1)	2	56,919,993	63,032,165	6,112,172		Female	<i>de novo</i> , parental allele NI	Affymetrix Genome-Wide Human SNP Array 6.0 (*)	Paternal del at Xp22.31 (1.4 Mb)
Case_2	2	57,606,726	59,619,316	2,012,590		Male	<i>de novo</i> , parental origin ND	Affymetrix CytoScan 750K Array, hg19	<i>de novo</i> 12p11.21-q11 del (6.5 Mb)**; <i>de novo</i> 2p16.1 BCL11A intronic del (17 Kb), 2p16.1 intergenic del (22.55 Kb)
de Leeuw et al. 2008	2	58,216,217	61,667,426	3,451,209	min del	Male	<i>de novo</i> , parental origin ND	Fine mapping by qPCR in Florisson paper (*)	Mosaic del 2p15-16.1 (20/30 cells observed with deletion)
		58,024,114	61,873,699	3,849,585	bal				
Florisson et al. 2013 (2)	2	58,714,795	65,392,528	6,677,733	min del	Female	<i>de novo</i> , parental origin ND	Affymetrix 250K Nsp1 SNP array, fine mapping by qPCR	None reported
		58,685,038	65,440,018	6,754,980	bal				
Case_3	2	59,017,244	64,379,673	5,362,429		Male	<i>de novo</i> , paternal allele deleted	Affymetrix Cytogenetics Whole-Genome 2.7M Array	No additional pathogenic CNVs Reported
Felix et al. 2010	2	59,139,200	62,488,871	3,349,671		Female	<i>de novo</i> , paternal allele deleted	Affymetrix Genome-Wide Human SNP Array 6.0	None reported
Liang et al. 2009	2	59,241,620	62,385,716	3,144,096		Female	<i>de novo</i> , paternal allele deleted	Agilent Human Genome CGH Microarray Kit 105A	Polymorphic inversion of chr 9
Balci et al. 2015/Basak et al. 2015 (3)	2	59,958,420	60,834,298	875,878	min del	Female	<i>de novo</i> , parental origin ND	Agilent 180K oligonucleotide array	None reported
		59,939,228	60,856,351	917,123	bal				
Basak et al. 2015 (2)	2	60,029,857	61,059,383	1,029,526		NA	<i>de novo</i> , parental origin ND	Human CytoSNP-12 BeadChips (Illumina)	None reported
Jorgez et al. 2014 (4)	2	60,066,496	66,376,496	6,310,000		Male	<i>de novo</i> , parental origin ND	SignatureChipOS v3.0	None reported
Ottolini et al. 2015	2	60,118,706	61,800,462	1,681,756		Female	<i>de novo</i> , parental origin ND	Not mentioned	None reported
Piccione et al. 2012 (2)	2	60,257,496	62,762,496	2,505,000		Male	<i>de novo</i> , parental origin ND	Agilent Human Genome CGH 244A array	<i>de novo</i> Xq28 del (29 kb)
Piccione et al. 2012 (1)	2	60,603,496	61,246,496	643,000		Female	<i>de novo</i> , paternal allele deleted	Agilent Human Genome CGH 44K array	Paternal 6q12 del (930 Kb)
Case_4	2	60,650,589	61,621,631	971,042		Female	<i>de novo</i> , parental origin ND	Affymetrix CytoScan 750K Array, hg19	No additional pathogenic CNVs Reported
Huchtagowder et al. 2012	2	60,672,255	63,144,695	2,472,440		Female	<i>de novo</i> , parental origin ND	Affymetrix Genome-Wide Human SNP Array 6.0	None reported
					min del reported	Male	<i>de novo</i> , parental origin ND	EmArray Cyto6000 v.2 (Emmory University)	2q13 del (343 Kb) and 6p25.3 del (80 Kb), unknown origin
Peter et al. 2014	2	60,689,299	60,830,491	141,192		Male	<i>de novo</i> , parental origin ND		
				203,000					Large run of homozygosity (ROH) on proximal side of 2p deletion, extends to ~61,809,113 bp (supplemental figure S1), negative testing for fragile X and Rett syndromes (MECP2)
Hancarova et al. 2013b / Basak et al. 2015 (1)	2	60,689,977	61,127,979	438,002		Female	<i>de novo</i> , paternal allele deleted	Illumina Human CytoSNP-12 BeadChip array, fine mapping of proximal bpt by MLPA	
Jorgez et al. 2014 (5)	2	61,056,496	65,656,496	4,600,000		Male	<i>de novo</i> , parental origin ND	SignatureChipOS v2.0 (135K)	None reported
Case_5	2	61,060,687	65,653,379	4,592,692		Male	<i>de novo</i> , parental origin ND	Signature Genomics SignatureChipOS™	No additional pathogenic CNVs Reported
Jorgez et al. 2014 (3)	2	61,126,496	63,516,496	2,390,000		Male	<i>de novo</i> , parental origin ND	SignatureChipOS v1.0 (105K)	None reported
Chabchoub et al. 2008	2	61,203,258	61,786,583	583,325		Male	<i>de novo</i> , parental origin ND	Affymetrix CytoScan 750K Array, hg19 (*)	None Reported, Negative testing for Marfan syndrome (FBN1) and Williams-Beuren (ELN)
Case_6	2	61,438,499	61,797,959	359,460		Male	<i>de novo</i> , parental origin ND	Affymetrix Genome-Wide Human SNP Array 6.0	No additional pathogenic CNVs Reported
Shimojima et al. 2015 (1)	2	61,495,220	61,733,075	237,855		Male	<i>de novo</i> , parental origin ND	Agilent 60 K Human Genome CGH Microarray	None reported
									Fragile site at 12q13.2 (benign variant), maternal 9p24.3 dup (493,399 Kb), maternal 9p24.3 dup (408,965 Kb), paternal 17q25.3 dup (656,833 Kb)
Fannemel et al. 2014	2	61,500,346	61,733,075	232,729		Male	<i>de novo</i> , parental origin ND	Agilent 180K SurePrint G3 Human CGH	
Jorgez et al. 2014 (6)	2	61,566,496	64,316,496	2,750,000		Male	<i>de novo</i> , parental origin ND	Exon targeted 180K Oligo array (BCM V.8)	None reported
Case_7	2	61,585,906	64,253,124	2,667,218		Male	<i>de novo</i> , maternal allele deleted	Affymetrix Cytogenetics Whole-Genome 2.7M Array	No additional pathogenic CNVs Reported
Shimojima et al. 2015 (2)	2	61,618,699	65,142,743	3,524,044		Female	undetermined	Agilent 60 K Human Genome CGH Microarray	None reported
Ronzoni et al. 2015	2	61,659,957	61,762,873	102,916		Male	<i>de novo</i> , parental origin ND	Agilent 180K	None reported

Genomic data are based on hg19 assembly.

Florisson et al. 2013 - Breakpoints calculated based on qPCR data in Table 1 and Table SI in paper.

NI - non informative

ND - not determined

* Updated breakpoints from original report, arrays re-run for cases have highest resolution array reported

** Case 2 also had a secondary CNV of 6.5Mb (de novo deletion of 12q pericentromeric region). The coding part of this CNV was 1.5Mb and included 11 reference genes and 4 OMIM genes, only one of which was bioinformatically predicted to be haploinsufficient (DNM1L). The OMIM genes were associated with phenotypes not noted in the patient namely lethal encephalopathy due to defective mitochondrial and peroxisomal fission (DNM1L), Charcot-Marie-Tooth disease type 4H (CMT4H) (FGD4), arrhythmogenic right ventricular cardiomyopathy (PKP2), myopathy, lactic acidosis, and sideroblastic anemia (YARS2). The EEG test for this patient was normal, excluding the role of PKP2, and the role of other genes based on the phenotypes is not likely but cannot be excluded.

Supplemental Table 3 – DNA repeated (RMSK) elements in regions flanking 2p15p16.1 deletions.

Deletion Flank				RMSK Element						
Chr	Start	Stop	Case_Flank	Family	Class	Name	Start	End	strand	Size (bp)
chr2	55675599	55676099	Case_1_distal	L1	LINE	L1MC4a	55675474	55676356	-	882
chr2	59619316	59619816	Case_2_proximal	ERV1-MaLR	LTR	THE1D	59619754	59620128	-	374
chr2	64379673	64380173	Case_3_proximal	L1	LINE	L1MEd	64379813	64380363	-	550
chr2	64379673	64380173	Case_3_proximal	L1	LINE	L1M5	64379554	64379772	-	218
chr2	61621631	61622131	Case_4_proximal	Alu	SINE	AluJb	61621499	61621693	+	194
chr2	61060188	61060688	Case_5_distal	Alu	SINE	AluJb	61060472	61060559	+	87
chr2	61060188	61060688	Case_5_distal	MIR	SINE	MIR	61060605	61060709	+	104
chr2	61438000	61438500	Case_6_distal	Alu	SINE	AluJb	61437854	61438072	-	218
chr2	61797959	61798459	Case_6_proximal	Alu	SINE	AluSp	61798046	61798342	-	296
chr2	61797959	61798459	Case_6_proximal	Alu	SINE	FRAM	61797931	61797967	-	36
chr2	61797959	61798459	Case_6_proximal	L1	LINE	L1MC4	61797984	61798046	+	62
chr2	61797959	61798459	Case_6_proximal	L1	LINE	L1MC4	61798342	61798364	+	22
chr2	61797959	61798459	Case_6_proximal	Alu	SINE	AluSg4	61798369	61798668	+	299
chr2	61585407	61585907	Case_7_distal	L1	LINE	L1MB4	61585365	61585565	+	200
chr2	61585407	61585907	Case_7_distal	L1	LINE	L1MB4	61585567	61586788	+	1221
chr2	64253124	64253624	Case_7_proximal	L2	LINE	L2a	64253622	64253756	+	134
chr2	64253124	64253624	Case_7_proximal	L2	LINE	L2a	64253123	64253196	+	73
chr2	64253124	64253624	Case_7_proximal	L2	LINE	L2a	64253483	64253546	+	63
chr2	61739267	61739767	Case_8_distal	L1	LINE	L1M5	61739735	61739895	+	160
chr2	55615646	55616146	Florisson-2013-1_distal	L2	LINE	L2a	55615767	55615850	+	83
chr2	55615646	55616146	Florisson-2013-1_distal	Low_complexity	Low_complexity	AT_rich	55616074	55616123	+	49
chr2	62362249	62362749	Florisson-2013-1_proximal	MIR	SINE	MIRb	62362209	62362422	+	213
chr2	62362249	62362749	Florisson-2013-1_proximal	Alu	SINE	AluY	62362489	62362784	-	295
chr2	63519476	63519976	Rajcan-Separovic-2007-2_proximal	L1	LINE	L1M4c	63519861	63521356	+	1495

chr2	56852663	56853163	Prontera-2010_distal	ERVL	LTR	LTR33A	56852798	56853220	-	422
chr2	60380981	60381481	Prontera-2010_proximal	ERVL-MaLR	LTR	MLT1F2	60380678	60381217	-	539
chr2	60380981	60381481	Prontera-2010_proximal	L2	LINE	L2a	60381300	60381435	-	135
chr2	56919494	56919994	Rajcan-Separovic-2007-1_distal	L1	LINE	L1PREC2	56919183	56920080	-	897
chr2	63032165	63032665	Rajcan-Separovic-2007-1_proximal	L1	LINE	L1ME4a	63032167	63032640	+	473
chr2	63032165	63032665	Rajcan-Separovic-2007-1_proximal	hAT-Charlie	DNA	MER1B	63031826	63032167	+	341
chr2	63032165	63032665	Rajcan-Separovic-2007-1_proximal	Alu	SINE	AluSz	63032659	63032949	-	290
chr2	58215717	58216217	deLeeuw-2008_distal	ERVL	LTR	MLT2B2	58215515	58216042	+	527
chr2	61667426	61667926	deLeeuw-2008_proximal	Alu	SINE	AluSq2	61667653	61667952	-	299
chr2	58714295	58714795	Florisson-2013-2_distal	ERV1	LTR	LTR27	58714137	58714616	-	479
chr2	59138700	59139200	Felix-2010_distal	Simple_repeat	Simple_repeat	(TG)n	59138982	59139028	+	46
chr2	62488871	62489371	Felix-2010_proximal	Alu	SINE	AluSx3	62488796	62489058	+	262
chr2	62488871	62489371	Felix-2010_proximal	ERV1	LTR	LTR49-int	62489058	62489255	-	197
chr2	62385716	62386216	Liang-2009_proximal	L1	LINE	L1M4b	62385941	62386419	+	478
chr2	60256997	60257497	Piccone-2012-2_distal	MIR	SINE	MIRb	60257339	60257530	-	191
chr2	62762496	62762996	Piccone-2012-2_proximal	ERV1	LTR	LTR12F	62762587	62763076	-	489
chr2	60602997	60603497	Piccone-2012-1_distal	ERVL	LTR	LTR16A	60603042	60603467	-	425
chr2	61246496	61246996	Piccone-2012-1_proximal	L1	LINE	L1M5	61246365	61247111	-	746
chr2	60671756	60672256	Huchtagowder-2012_distal	L2	LINE	L2a	60672083	60672212	+	129
chr2	63144695	63145195	Huchtagowder-2012_proximal	Alu	SINE	AluSz	63145033	63145331	-	298
chr2	63144695	63145195	Huchtagowder-2012_proximal	ERVL	LTR	LTR40c	63144876	63144974	-	98
chr2	63144695	63145195	Huchtagowder-2012_proximal	MIR	SINE	MIRc	63144639	63144711	-	72
chr2	60689478	60689978	Hancarova-2012_distal	MIR	SINE	MIR3	60689893	60689972	+	79
chr2	61127979	61128479	Hancarova-2012_proximal	Alu	SINE	AluSq2	61128279	61128595	-	316
chr2	61202758	61203258	Chabchoub-2008_distal	Alu	SINE	AluSx1	61202886	61203196	-	310
chr2	61202758	61203258	Chabchoub-2008_distal	MIR	SINE	MIRb	61203230	61203342	+	112
chr2	61786583	61787083	Chabchoub-2008_proximal	Alu	SINE	AluJr	61786377	61786593	-	216

chr2	61786583	61787083	Chabchoub-2008_proximal	Alu	SINE	AluSx3	61786653	61786948	+	295
chr2	61786583	61787083	Chabchoub-2008_proximal	Alu	SINE	AluY	61786950	61787253	+	303
chr2	61499846	61500346	Fannemel-2014_distal	L2	LINE	L2	61499566	61499856		290
chr2	61733075	61733575	Fannemel-2014_proximal	Alu	SINE	AluSz	61733275	61733575		300
chr2	61733075	61733575	Fannemel-2014_proximal	Simple_repeat	Simple_repeat	(TAAA)n	61733225	61733249		24

This table contains the Repeated Elements by RepeatMasker - <http://www.repeatmasker.org/> - (RMSK) that overlap with regions flanking 2p15p16.1 microdeletions (500 bp upstream & downstream). Genomic positions for the regions flanking each deletion (proximal or distal) are provided along with the case identifier. A total of 56 RMSK elements are listed along with their corresponding Family, Class, Name, Start, End, strand, and size (bp). The UCSC rmsk track includes up to ten different classes of repeats: short interspersed nuclear elements (SINE), which include ALUs, long interspersed nuclear elements (LINE), long terminal repeat elements (LTR), which include retroposons, DNA repeat elements (DNA), simple repeats (micro-satellites), low complexity repeats, satellite repeats, RNA repeats (including RNA, tRNA, rRNA, snRNA, scRNA, srpRNA), other repeats, which includes class RC (Rolling Circle), and a category labeled unknown. Genome assembly build used is Human Feb. 2009 (GRCh37/hg19).

B3GNT2	mRNA	+	+	+	+	+	+	+	+	+	+	+	+	+	+	+	16	48.5		36.11
MIR5192	ncRNA	+	+	+	+	+	+	+	+	+	+	+	+	+	+	+	16	48.5		
TMEM17	mRNA	+	+	+	+	+		+	+		+	+	+	+	+	+	14	42.4	37.90%	32.65
EHBP1	mRNA	+	+	+	+	+		+		+	+	+	+	+	+	+	13	39.4	43.60%	2.88
AC009501.4	ncRNA	+	+		+	+		+			+	+	+	+	+	+	11	33.3		
OTX1	mRNA	+	+		+	+		+			+	+	+	+	+	+	11	33.3	63.70%	7.55
DBIL5P2	ncRNA	+	+		+	+		+			+	+	+	+	+	+	11	33.3		
WDPCP	mRNA	+	+		+	+		+		+	+	+	+	+	+	+	11	33.3		24.69
MDH1	mRNA	+			+	+		+			+	+		+	+	+	9	27.3	53.40%	5.43
UGP2	mRNA	+			+	+		+			+	+		+	+	+	9	27.3	1.70%	6.89
VPS54	mRNA	+			+	+		+			+	+		+	+	+	9	27.3	41.60%	7.35
PELI1	mRNA	+			+	+		+			+	+				+	7	21.2	6.20%	7.26
LINC00309	ncRNA	+			+			+			+	+				+	6	18.2		
LGALS1	mRNA	+			+			+			+	+				+	6	18.2		25.04
AFTPH	mRNA	+			+			+			+	+				+	6	18.2	17.80%	20.39
MIR4434	ncRNA	+			+			+			+	+				+	6	18.2		
AC007365.1	ncRNA	+			+			+			+	+				+	6	18.2		
SERTAD2	mRNA	+			+			+			+	+				+	6	18.2	7.80%	27.45
AC007880.1	ncRNA	+			+			+			+	+				+	6	18.2		
AC007386.2	ncRNA	+			+			+			+	+				+	6	18.2		
SLC1A4	mRNA	+			+			+			+	+					5	15.2	69.00%	39.21
CEP68	mRNA				+			+			+	+					4	12.1	92.90%	83.58
RAB1A	mRNA				+			+			+	+					4	12.1	10.70%	3.32
ACTR2	mRNA							+			+	+					3	9.1	31.10%	8.79
SPRED2	mRNA							+			+	+					3	9.1	18.80%	17.57

+ Gene included

(+) Gene possibly included based on data, not included in count

+ (in red color): Gene disrupted by the breakpoint

Non-coding RNA gene (ncRNA)

Protein coding gene (mRNA)

Bold – 16 genes deleted in >50% of cases

* From Huang et al. 2010 Supplementary Table 2

Supplemental Table 5 – A summary of known functions and mutations of genes deleted in >50% of cases and their animal knockout model reports.

Gene	Function (PubMed ID)		Other variants	Animal knockout model (PubMed ID)		
	Main biological role(s)	Brain/neuronal-related function(s)	No. of reported mutations in HGMD [phenotypes (PubMed ID)]	Mouse (MGI or PubMed)	Zebrafish	Other
<i>VRK2*</i>	Encodes a serine/threonine protein kinase that modulates several signaling pathways including p53 signaling pathway and tumor cell growth (16704422). It acts as the negative-regulator of apoptosis (23449449).	VRK2 acts as a modulator of accumulation of misfolded polyglutamine (polyQ) aggregation and toxicity in early stages of neurodegenerative disease progression by negative regulation of the chaperonin (CCT4) stability (24298020) through inhibiting USP25 deubiquitinase (25755282).	–	–	–	–
<i>FANCL*</i>	Encodes a ubiquitin ligase that ubiquitinates FANCD2 which is an essential step in the FA pathway of DNA repair (19423727).	–	11 [Fanconi anemia, autosomal recessive (24459294; 23613520; 25754594; 19405097; 22720145; 12973351)]	abnormal male/female reproductive system and infertility; decreased embryo weight and complete prenatal/embryonic lethality (12417526)	Mutations in <i>fancl</i> in zebrafish leads to sex reversal by Tp53-mediated germ cell apoptosis, but no major phenotypic abnormalities are observed (21951543, 20661450).	Drosophila: Knockdown of FANCL results in viable and fertile flies with specific hypersensitivity to cross-linking agents and hence DNA repair deficiency (16860002).
<i>BCL11A</i>	Encodes a zinc-finger protein which functions as a myeloid and B-cell proto-oncogene. It is associated with leukemogenesis and hematopoiesis and has been identified as a negative regulator of fetal hemoglobin (26125973, 26080908, 26019277, 25938782).	BCL11A have recently been associated with proper migration of cortical projection neurons and neurodevelopment (26182416, 26019277, 25938782)	2 [Increased fetal hemoglobin levels (24115442); Autism (22542183)]	Abnormal immune-system morphology including decreased level of B-cells/T-cells/leukocytes ,abnormal humoral immune response ; abnormal hematopoiesis, erythropoiesis and decreased hemoglobin content; Abnormal neuronal/axon morphology and/or differentiation, complete neonatal lethality	–	–
<i>PAPOLG</i>	Encodes a member of the Poly(A) polymerase family which mediate the post-transcriptional addition of poly(A) tail to the 3' end of mRNA precursors and several small RNAs.	Unknown	–	–	–	–
<i>REL</i>	Encodes c-Rel protein which is a proto-oncogene and a member of the NF-κB family of transcription factors . It acts as a crucial regulator of B and T cell function (22207895).	c-Rel is known for its neuroprotective and anti-apoptotic role in NF-κB pathway (26042083, 19094066) and is required for hippocampal long-term synaptic plasticity and memory formation (24854662).	–	Abnormal immune-system morphology including decreased level of B-cells/T-cells, abnormal levels of IgG/IgM/IgE/macrophages and cytokine secretion; abnormal DNA replication and cell cycle; increased neuron apoptosis; abnormal skeleton morphology premature death (26042083).	–	–
<i>PUS10</i>	Encodes a pseudouridylylase synthase which catalyzes the isomerization of uridine to pseudouridine of RNAs (23743107). Also, act as RNA chaperones, assisting with proper tRNA folding and assembly (16920741, 23743107).	Unknown	–	–	–	–
<i>PEX13</i>	Encodes a peroxisomal membrane protein which has an important role in peroxisomal biogenesis (23716570).	–	10 [Zellweger syndrome, autosomal recessive (21031596; 25525159; 10332040; 17041890; 23716570; 19449432; 11405337); Neonatal adrenoleukodystrophy, autosomal recessive (10332040)]	abnormal/thin cerebellum and cerebral cortex development, postnatal growth retardation and decreased body weight , hypotonia, impaired coordination, impaired reflex and limb grasping , neuronal abnormalities including astrocytosis, gliosis, and neuron degeneration, premature death and complete neonatal lethality	No major phenotypic abnormalities due to ineffective knockdown (20556416)	–
<i>KIAA1841</i>	Encodes an uncharacterized protein KIAA1841	Unknown	–	–	–	–
<i>C2orf74</i>	Encodes an uncharacterized protein, chromosome 2 open reading frame 74.	Unknown	–	–	No orthologue	–
<i>AHSA2</i>	Encodes a protein acting as a co-chaperone of heat shock protein 90 (Hsp90) and is associated with ATPase activator activity.	Unknown	–	decreased total retina thickness	No orthologue	–

USP34	Encodes a deubiquitinating enzyme which acts as the regulator of axin stability and Wnt/beta-catenin signaling pathway (21383061) as well as the negative regulator of NF-kB pathway (23590831, 25027767). It also functions as promoter of genome stability by regulating ubiquitin signaling at DNA double-strand breaks (23863847).	Unknown	1 [Congenital heart disease (23665959)]	Early lethality in mice (prior to 4 weeks of age). Surviving mice grew poorly and exhibited numerous neurological abnormalities (26273529).	-	Drosophila: knock down results in early lethality (22937016).
XPO1	Encodes an exportin protein (XPO1/CRM1) that mediates export of ~200 leucine-rich nuclear export signal (NES)-bearing proteins and of RNAs from nucleus to cytoplasm (9384386). It is also involved in mitotic microtubule spindle (kinetochore) regulation and assembly (26196321; 25982429).	Nucleocytoplasmic shuttling mediated by XPO1 is reported for molecules relevant for synaptogenesis (23383123) and neuronal positioning in brain (17062576). These proteins normally function in cytoplasm.	-	-	-	Drosophila: knockdown results in nuclear accumulation of expanded polyglutamine (polyQ) protein aggregates leading to neural cell toxicity and neurodegenerative diseases (21300695).
FAM161A	Encodes a protein with restricted activity to mature photoreceptors in the retina.	Unknown	11 [Retinitis pigmentosa, autosomal recessive (20705278, 25097241, 22581970, 20705279); Retinal dystrophy (23167750); Retinal degeneration (26352687)]	abnormal vision/retinal photoreceptor morphology and their degeneration; microgliosis; abnormal cilium morphology (24833722)	-	-
CCT4	Encodes a molecular chaperone which facilitates proper folding of proteins upon ATP hydrolysis e.g. actin and tubulin (23612981, 10604479).	-	-	-	-	Rat: Mutation in Cct4 is associated with recessive hereditary sensory neuropathy (12874111; 25124038) and cutaneous nerve degeneration (15193290)
COMMD1	Encodes a regulator of copper homeostasis, sodium uptake, and NF-kB signaling (24080195). It acts as the negative regulator of NF-kB activity by promoting ubiquitination and the subsequent proteasomal degradation of NF-kB role-player, RELA (15799966, 20048074). Diseases associated with COMMD1 include Wilson disease and copper toxicosis (autosomal recessive disorders) characterized by accumulation of copper in the liver (22216203).	Change in the expression of COMMD1 affects brain metal-ion homeostasis by influencing intracellular zinc concentrations due to abnormal copper levels. This is believed to affect autism-associated pathways at excitatory synapses (25007851). COMMD1 is also known as a regulator of misfolded protein aggregation involved in neurodegenerative disorders e.g. Amyotrophic Lateral Sclerosis (ALS) and Parkinson's (24691167). Heterozygous deletion of COMMD1 has no phenotype, but homozygous deletion associated with high functioning autism (21658582)	1 [Elevated urinary copper (20550661)]	abnormal brain development, embryonic growth retardation and decreased size, abnormal embryo turning, abnormal allantois morphology, abnormal placenta vasculature, complete prenatal lethality (17371845), increased liver copper level (22216203)	-	Dog: Increased liver copper level and hepatitis (25053573; 22879914)

HGMD: The Human Gene Mutation Database - a catalogue of human gene mutation studies with their reported phenotypic features (Accessed at: <http://www.hgmd.cf.ac.uk/ac/index.php>)

MGI: Mouse Genome informatics database - a catalogue of mouse gene knockout studies with their reported phenotypic features (Accessed at: <http://www.informatics.jax.org/>)

*These genes were not deleted in >50% of cases but included here as we included in our candidate list due to their isolated involvement in two CNVs/cases

Supplemental Table 6 – Positive VISTA enhancer elements in the 2p15p16.1 deletion region.

Chromosome Position	element #	Expression Pattern Location [observed embryos/total embryos]
chr2:58748340-58750140	1174	dorsal root ganglion[6/6]
chr2:58799729-58800607	1071	ear[4/10]
chr2:58859997-58861674	1152	limb[4/5]
chr2:58975738-58977115	1067	dorsal root ganglion[3/7], limb[5/7]
chr2:59102071-59103380	1199	other[3/6]
chr2:59178992-59180242	1181	heart[3/8]
chr2:59198905-59200529	393	eye[6/12]
chr2:59304974-59306893	975	midbrain (mesencephalon)[4/7]
chr2:59476604-59477955	1119	neural tube[6/6], hindbrain (rhombencephalon)[5/6]
chr2:59540640-59541937	836	facial mesenchyme[5/12]
chr2:59746377-59746992	394	midbrain (mesencephalon)[4/11]
chr2:60352514-60353602	779	midbrain (mesencephalon)[8/9], forebrain[5/9]
chr2:60441495-60442515	399	forebrain[5/7]
chr2:60498057-60502013	1535	hindbrain (rhombencephalon)[4/5]
chr2:60761404-60763073	957	forebrain[4/4]
chr2:60855056-60856888	1142	hindbrain (rhombencephalon)[3/3]
chr2:63193855-63194929	690	midbrain (mesencephalon)[7/11]
chr2:63275695-63277103	1066	hindbrain (rhombencephalon)[5/5], midbrain (mesencephalon)[5/5], forebrain[5/5]
chr2:66297527-66299214	205	genital tubercle[8/9]

Bold: Brain/neural-expressed enhancers

This table contains the 19 positive enhancer elements found in the 2p15p16.1 region and includes their chromosomal position (chr:start-stop), element number, and observed expression pattern location in mouse embryos. The elements are listed in order of their position in the 2p15p16.1 deletion region from distal (telomeric) to proximal (centromeric).

Supplemental Table 7 – Enriched pathways for the 16 most commonly deleted genes in the 2p15p16.1 microdeletion region.

Pathway Name	#Gene	EntrezGene	Statistics
Canonical NF-kappaB pathway	2	<i>XPO1, REL</i>	C=35;O=2;E=0.01;R=164.29;rawP=6.67e-05;adjP=0.0020
Endogenous TLR signaling	2	<i>XPO1, REL</i>	C=57;O=2;E=0.02;R=100.88;rawP=0.0002;adjP=0.0020
CD40/CD40L signaling	2	<i>XPO1, REL</i>	C=58;O=2;E=0.02;R=99.14;rawP=0.0002;adjP=0.0020
IL23-mediated signaling events	2	<i>XPO1, REL</i>	C=66;O=2;E=0.02;R=87.13;rawP=0.0002;adjP=0.0020
Aurora A signaling	2	<i>XPO1, REL</i>	C=64;O=2;E=0.02;R=89.85;rawP=0.0002;adjP=0.0020
IL2 signaling events mediated by PI3K	2	<i>XPO1, REL</i>	C=67;O=2;E=0.02;R=85.82;rawP=0.0002;adjP=0.0020
Signaling events regulated by Ret tyrosine kinase	2	<i>XPO1, REL</i>	C=69;O=2;E=0.02;R=83.34;rawP=0.0003;adjP=0.0026
IL12-mediated signaling events	2	<i>XPO1, REL</i>	C=113;O=2;E=0.04;R=50.89;rawP=0.0007;adjP=0.0033
IL2-mediated signaling events	2	<i>XPO1, REL</i>	C=115;O=2;E=0.04;R=50.00;rawP=0.0007;adjP=0.0033
LPA receptor mediated events	2	<i>XPO1, REL</i>	C=100;O=2;E=0.03;R=57.50;rawP=0.0005;adjP=0.0033

15/16 genes were recognized by Webgestalt. This table lists the top 10 pathways for the WebGestalt pathway commons enrichment analysis. The first column lists the pathway, the second and third columns indicate the number and gene identification for the genes involved, and the last row contains the statistics from the enrichment analysis: number of reference genes in the category (C), number of genes in the gene set and also in the category (O), expected number in the category (E), Ratio of enrichment (R), p value from hypergeometric test (rawP), and p value adjusted by the multiple test adjustment (adjP).

Supplemental Table 8 – Sequence of morpholinos used to knockdown the genes of interest in zebrafish.

Human gene	Zebrafish orthologue (Zv9)	Type of MO : (Sequence (5'→ 3'))	Target site
<i>XPO1</i>	<i>xpo1a</i>	SB: (TCAGAAACTGTGGAAGAAGCCAGAA)	i8-e9 boundary
	<i>xpo1b</i>	SB: (AAAATGATCTTACTTACCTGTGGCC)	e1-i1 boundary
<i>USP34</i>	<i>usp34</i>	SB: (GCCTTAATGAGTGCTACTGACCTCT)	e2-i2 boundary
<i>REL</i>	<i>rel</i>	SB: (AAAGATTGAACTTACGCAATGGCCC)	e4-i4 boundary (did not work)
	<i>rel</i>	SB: (GTATAAATACTCGTACTCACCATCC)	e1-i1 boundary (did not work)
	<i>rel</i>	TB: (TTGAGAGGGATTGCACATCCATAAC)	translation initiation site
<i>BCL11A</i>	<i>bcl11aa</i>	SB: (TGTCTTTACTTACGCGAAAAATCCC)	e1-i1 boundary
	<i>bcl11ab</i>	SB: (AGAACTTTCCGGTAACTTACGCGAA)	e1-i1 boundary
<i>VRK2</i>	<i>vrk2</i>	SB: (AAGTCAATCTCATACTTGTTCGGT)	e4-i4 boundary
<i>FANCL</i>	<i>fancl</i>	SB: (CCACTTGATTTATTGTACCTGCTTC)	e3-i3 boundary
	MM-control	SB: (TCACAAACTCTCGAACAACCCAGAA)	No binding site
	<i>p53</i>	TB: (GCGCCATTGCTTTGCAAGAATTG)	translation initiation site

Abbreviations: MO = morpholino; SB = Splice-blocking; TB = Translation-blocking; i: intron; e: exon; MM = gene mismatch

Supplemental Table 9 – Sequence of PCR primers used to confirm the knockdown of the genes of interest in zebrafish.

Zebrafish gene	Forward primer (Sequence (5'→ 3'))	Reverse primer (Sequence (5'→ 3'))	Primer binding site	Annealing temperature
<i>xpo1a</i>	CAGAATGCCCTCTGGTTCA	TAGCAGCATGTAGTGCAGGG	F: e8, R: e11	57.0 °C
<i>xpo1b</i>	GACAATGTTAGCCGACCACG	TGCGACTTGCACCCACAATA	F: e1, R: e6	56.0 °C
<i>rel*</i>	-	-	-	-
<i>usp34</i>	ATGTGTGAGAACTGCGCCGA	AAAGCAGCGTAGACCCGTTT	F: e1, R: e3	52.9 °C
<i>bcl11aa</i>	ATCTTCCCTGCGCCATCTTT	GCCATTGCACTGCTTCCTTT	F: 5' UTR, R: e2	55.0 °C
<i>bcl11ab</i>	CCATGAAGCCCAACACAAGC	ATGTCGGCCAAAGGAAACCT	F: 5' UTR, R: e2	53.5 °C
<i>vrk2</i>	GTCCCTGTTGAGATGATGCT	GTACACCCAATTGTAGCACGC	F: e2, R: e5	57.0 °C
<i>fancl</i>	TGAGCTGCTTGCTGATGAGA	ACTGACATCCTGGTTGGCTC	F: e1, R: e5	53.0 °C
<i>Actb2 (b-actin2)**</i>	GCAGAAGGAGATCACATCCCTGGC	CATTGCCGTCACCTTCACCGTTC	F: e4, R: e5	52.0 °C

Abbreviations: e = exon; i = intron; F = Forward; R = Reverse; UTR = Untranslated region

**rel* knockdown was not successful with two independently designed splice-blocking morpholinos, therefore translation-blocking morpholino was used and knockdown was confirmed with western-blotting.

**primer sequences for *Actb2* were obtained from Casadei et al., (2011) (PMID: 21281742) and were used as the housekeeping gene control